Multi-Band Hybrid Active-Passive Radar Sensor Fusion

Piers J. Beasley, Matthew A. Ritchie*
Department of Electronic and Electrical Engineering
University College London
London, UK
{piers.beasley.19} {m.ritchie}* @ucl.ac.uk

***Abstract*—In this paper the topic of joint active and passive (hybrid) radar detection is introduced and the theoretical benefits are outlined. An experimental hybrid radar setup is presented where a low-cost Software Defined Radio (SDR) based radar system is used for hybrid sensing of targets using active and Passive Bistatic Radar (PBR). Experimental results are presented for simultaneously sensing using an active 2.4 GHz radar and 690 MHz Digital Video Broadcasting — Terrestrial (DVB-T) based PBR mode. The detection performance of each sensor and a joint sensor performance are evaluated, where the joint detection performance is found to exceed that of the individual sensors alone. The ability to reduce active radar transmissions, but still retain a reasonable detection performance, is investigated using experimental data and the case is made for adaptive behaviour in order to exploit the benefits available to hybrid radars.**

***Index Terms*—Hybrid Radar, Multistatic Radar, Passive Radar, Passive Bistatic Radar, Software Defined Radio, Software Defined Radar**

I. Introduction

Hybrid radar is a new paradigm of radar that exploits both active radar and Passive Bistatic Radar (PBR), capitalising on the strengths of each sensor. The topic of hybrid radar is gaining more attention with papers starting to surface on the expected benefits from the hybrid architecture [1]–[3]. A summary of the main benefits of hybrid radar sensing are listed below:

1) Exploit the Benefits of Active and Passive Radar: A hybrid combination of active and passive radar capitalises on the strengths of passive radar (e.g. no transmitter cost, covert operation, spatial diversity), as well as the strengths of active radar (e.g. optimised waveform, transmitter beam-steering) [2].

2) Low-Probability of Intercept (LPI): In a hybrid system, the radar's active transmission power can be significantly lowered, should there be a strong and reliable passive source available [3]. Minimising active transmissions, and their respective strength, will reduce the probability of Electronic Support Measures (ESMs) detecting the radar while it is searching for a target or engaged in target tracking.

3) Enhanced Detection Probability: A hybrid system exploits the diversity in target back scatter from multiple target angles, a benefit intrinsic to multistatic radars. This can greatly improve the ability of a radar system in detecting stealth aircraft, that often have intentionally low Radar Cross Sections (RCS) for certain angles of incidence [4].

4) Resilience to Electronic Counter Measures: The passive element of the hybrid radar is inherently more resilient to jamming, than active radar, due to the jamming entity not being aware of the passive receivers location. Additionally, different central Radio Frequencies (RF) would likely be used for the active radar and passive radar, requiring the jamming entity to jam either a broad range of frequencies or multiple separate frequency bands. [4], [5].

In [2], Gao et al. propose a hybrid design comprising of an active array, used for active radar transmissions, and a receive array, used for detecting target echos from the active radar and an uncooperative Illuminator of Opportunity (IoO). Simulation results are presented that show a greater than 10 dB improvement in the signal-to-interference-plus-noise ratio (SINR), for the same active component signal-to-noise ratio (SNR), when an IoO is added to a conventional beamforming transmit (Tx) and receive system. A similar configuration is proposed by Kuschel et al. in [1], though the purpose of the research differs. Gao et al. investigate joint transmit and receive optimisation via beam-forming for the hybrid system, whereas [1] focuses on the fusion of multiple channels of radar target detections. The theory of a Deployable Multiband Passive/Active Radar for Air Defense (DMPAR) system architecture is presented by Fraunhofer in [1]. This system incorporates four RF Sensors: active high frequency e.g. S/X/C band; passive high frequency e.g. PBR nodes for S/X/C active nodes; active low frequency e.g. UHF/VHF; passive low frequency e.g. DVB-T, DAB, FM. It is suggested that through use of such a broad range of RF sensors the benefits of the individual sensors will compensate for sensor specific shortcomings [1]. In [1], [6] two methods for the fusion of individual RF sensor signals are described. An incoherent integration method, referred to as centralised detection, is presented that combines raw measurement data from each sensor at a centralised decision node, and secondary method of fusion is presented named decentralised fusion. In the decentralised method, individual sensors decide upon detections autonomously, these binary decisions are then combined at a central node. From the functional simulations described in [1], the centralised DMPAR concept yields superior performance in all the proposed scenarios. Furthermore,

This work is jointly funded as part of an iCASE PhD studentship by the Engineering and Physical Sciences Research Council (EPSRC) and UK Defence Science and Technology Laboratory (Dstl).

the centralised DMPAR has a detection range triple that of the single monostatic active radar itself. The less advanced decentralised method's simulation results still indicate a factor of two improvement in detection range over the active radar alone.

A physical implementation of a DMPAR system is realised in [7] to collect experimental results for comparison with the simulations in [1]. This paper describes four days of experimental trials in late 2014, named the DETOUR trials. The implementation used a combination of discrete active and passive radar systems to create a DMPAR system for tracking commercial aircraft. The analysis of fusion strategies for the trials data is presented in [6], for the two system configuration scenarios, co-located and distributed. The trials confirmed that the range improvement of co-located DMPAR configurations concur with simulated results, however, when using the distributed configuration, decentralised fusion outperformed the centralised fusion method, mainly in detection range.

In terms of practical implementations of hybrid radar systems, Software Defined Radios (SDRs) have been found to provide a good platform to perform the multiple functions in multiple frequency bands required in hybrid radar. This is achieved through rapid software reconfiguration of flexible RF hardware and the digital signal processing. The cost-efficiency and highly flexible nature of SDRs make their exploitation as multi-functional radar transceivers in hybrid radar very promising. In previous works by Ritchie et al., a high performance multi-role RF sensor based on a Xilinx Radio Frequency System on a Chip (RFSoC) is shown to work in a hybrid radar mode, sensing a human target at two different frequency bands [8]. Additionally, in previous works by this author, the development of a hybrid experimental radar system is presented, where multiple low-cost bladeRF SDRs are utilised for sensing a human and micro-drone target using active radar and Wi-Fi PBR [9].

This paper investigates the fusion of active and PBR radar detections using empirical radar data captured using a low-cost SDR based radar. A comparison is made between the active radar, PBR and fused active and passive (hybrid) radar detection performance. This paper additionally studies how a hybrid radar's active radar transmit power can be reduced, yet still sustain a reasonable overall hybrid radar detection performance.

In the following section, the experimental scenario in which the hybrid radar data were collected is presented. In section III, the signal processing used in the active and passive radar sensors is described. The experimental results are then analysed in section IV, before the conclusions and future work are detailed in the final section.

II. Experimental System and Scenario

In this section, details on the hybrid radar system, PBR IoO, experimental geometries, and radar targets are presented.

A. bladeRAD Hybrid Radar System

During the trial, the bladeRAD multi-functional radar system was used to simultaneously collect active and PBR data.

TABLE I
Hybrid Radar Capture Parameters

Radar Parameter	FMCW Active	DVB-T Passive
Central RF [GHz]	2.44	0.69
Sample Rate [MSPS]	60	20
Filtered BW [MHz]	30	8
PRF [kHz]	1	1
CPI [s]	0.5	0.5
Waveform	LFM Up-Chirp	OFDM (64-QAM)
Waveform BW [MHz]	30	7.61
Antenna Gain [dBi]	18 (Dish)	12.5 (Yagi)
Tx Power	0.2 W	170 kW

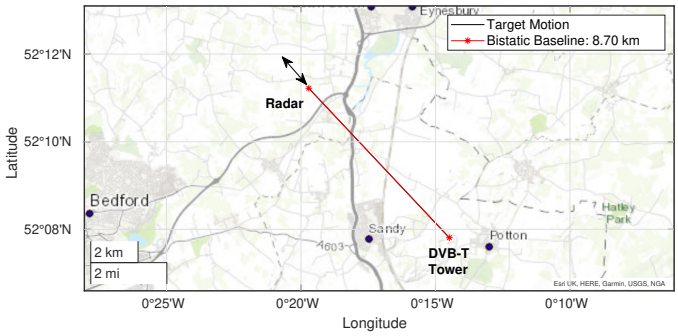

Fig. 1. Hybrid radar experimental geometry. The target moved back and forth from the radar with a PBR bistatic angle of $\beta = 0°$. In this figure, the extent of the target's motion has been exaggerated for clarity.

The bladeRAD system is a low-cost experimental hybrid radar system, developed from a combination of Nuand bladeRF micro 2.0 SDRs [9]. bladeRAD is a staring radar, thus currently does not provide target elevation or azimuth estimations. During the measurements, the active radar component was operated in an S-Band Frequency-Modulated-Continuous-Wave (FMCW) mode, with identical 18 dBi parabolic dish antennae used for the transmit and receive channels. For the PBR component, a non-cooperative DVB-T tower was used as an IoO. Table I details the key radar parameters for both the active and PBR sensors.

B. Experimental Scenario

The radar experiments were conducted in a field in Bedfordshire, UK. The PBR IoO was located in Sandy Heath, 8.696 km to the southeast, with an estimated antenna height of 292 meters above sea level. The trial location provided an uninterrupted line-of-sight to the DVB-T tower. Fig. 1 is a map illustrating the location of the radar, Sandy Heath DVB-T tower, and the motion of the target in relation to the PBR baseline. The targets were instructed to move back and forth from the radar, reaching a maximum range of 100 meters, with a bistatic angle of $\beta = 0°$ to allow direct comparison between the active and PBR data. The configuration of the radar is detailed in Fig. 2. As standard in many PBRs, one antenna is used for measuring the direct path signal from the DVB-T transmitter (reference channel), and another antenna is used for measuring target reflections (surveillance channel).

Two different targets were used during the radar experiments, a small DJI Phantom consumer drone, and a small

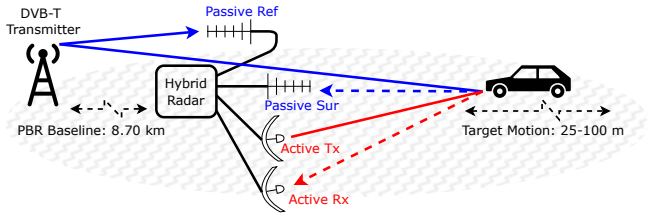

Fig. 2. bladeRAD hybrid radar experimental setup.

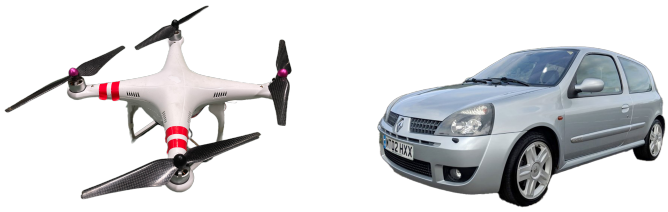

(a) Drone target (b) Car target

Fig. 3. Two different targets were used during the Hybrid radar experiments (a) DJI Phantom consumer quad-copter drone (b) Renault Clio car.

two-door Renault Clio car, photographed in Fig. 3a and Fig. 3b respectively. The small drone was retrofitted with carbon fibre propellers to increase the RCS of the propellers, improving the SNR of the drone micro-Doppler. Both targets position were logged, using a GPS logger, for the duration of the measurements to provide ground truth data for calculating empirical detection probabilities for each sensor.

III. Signal Processing

The bladeRAD experimental radar system digitises radar data straight to binary files for post-capture signal processing. The active and PBR sensors are triggered simultaneously, such that ADC, DACs and data clocks, are synchronised to ensure the two channels of radar data remain perfectly time aligned from the start to the end of the measurement.

A. Active FMCW Radar Signal Processing

Unlike in a conventional FMCW radar, where the receive channel is mixed (de-ramped) with the transmit channel at RF in hardware, the bladeRAD system digitally mixes the receive channel with a pre-recorded LFM chirp at baseband in software [9]. The de-ramped signal is then decimated, before conversion to the frequency domain via a Discrete-Fourier-Transform (DFT). The data is then reshaped into a 2D radar matrix, where each row represents an individual pulse's range profile (fast-time dimension). A Moving Target Indicator (MTI) filter is then operated down each column of the 2D radar matrix (slow-time dimension), to remove stationary/slow moving clutter [10]. Range-Doppler surfaces are subsequently formed via taking a DFT down each column of the slow-time dimension. For the results presented in this paper, a 0.5 second DFT Coherent Processing Interval (CPI) and 80 % overlap was used when forming the range-Doppler surfaces, resulting in approximately a 10 Hz radar update rate. Fig. 4 illustrates the high level processing flow of the active radar sensor.

B. Passive Bistatic Radar Signal Processing

The passive radar data was processed using a batched processing algorithm, as described by Bo Tan et al. in [11]. In conventional passive radar signal processing, the surveillance channel is cross-correlated with Doppler-shifted replicas of the reference channel, creating a matrix of range compression filters, each replica matched to a particular potential target Doppler velocity [12]. However, the batch signal processing approach is more analogous to active radar signal processing. In this approach, the reference and surveillance signals are split into n segments-per-second - where n is equivalent to an active radar's Pulse-Repetition-Frequency (PRF) - before then being cross-correlated to create a 2D radar matrix. Range-Doppler surfaces are again then formed using the same method and parameters as described in section III-A. For the low-Doppler targets and short target ranges the, considerably more computationally efficient, batched processing algorithm was found to suffice for PBR target detections. A fundamental challenge in PBR, results from the target echos being numerous orders of magnitude weaker than the direct signal path and static-clutter returns (multipath). The inherent inclusion of the direct-signal from the transmitter, in the surveillance channel, referred to as Direct-Signal-Interference (DSI), results in a extremely strong correlation response at zero range and Doppler. Additionally, multi-path returns from static clutter also result in strong correlation responses. The side lobes of the DSI and static-clutter returns are normally magnitudes stronger than the target returns, thus often mask short-range and low-Doppler targets. There are several signal processing techniques for compensating for the effects of DSI and clutter in PBR [13]. In this work, the batched-based CLEAN cancellation technique is used [14]. CLEAN is an iterative technique that operates, post-correlation, by estimating the strongest signal components in range-Doppler surfaces and then iteratively removing them. In the PBR data collected during this trial, on average, a 62.5 dB cancellation of DSI and clutter was observed using this technique, calculated by comparing the relative power of target cell to peak DSI or clutter cell. The CLEANed PBR range-Doppler surfaces were finally interpolated (using bicubic interpolation), such that range bin and Doppler bin sizes of the active radar and PBR sensors matched. Fig. 4 illustrates the high level processing flow of the PBR sensor.

C. CFAR Detection

In this work, decentralised information fusion was used to combine the active and PBR radar detections [1], [6], [15]. 2D Cell-Averaging (CA) Constant-False-Alarm-Rate (CFAR) detectors were used to determine detections in the individual active and PBR range-Doppler surfaces [16]. The binary output of the active and PBR CFAR detectors were then combined using a 1-of-k (OR) decision rule, such that a hybrid detection, H_{det}, was made when either the active radar A_{det} or PBR P_{det} made a detection.

$$H_{det} = A_{det} \vee P_{det} \tag{1}$$

A desired false alarm rate of $P_{fa} = 1 \times 10^{-6}$ was selected. This value was high enough to allow verification of the false alarm rate with the quantity of empirical data, however, low enough that it is very improbable that false alarms will result in false positives when calculating the empirical probability of detection, described in section III-D. In order to allow true comparison between the active, passive, and hybrid detector performance, the false alarm rate of each detector output must be kept constant. Therefore, the false alarm rate of the active and PBR CFAR detectors feeding the decentralised hybrid detector (P_{fai}), must be adjusted to be a factor of two smaller ($P_{fai} = 5 \times 10^{-7}$) in order for the hybrid detector to achieve an overall $P_{fa} = 1 \times 10^{-6}$. Identical properties were used for the active radar and PBR CA-CFAR detectors, namely 15 training cells and 3 guard cells.

D. Calculating Probability of Detection

In this work, a single empirical Probability of detection, P_d, metric was calculated for each measurement scenario. The P_d was calculated as the ratio of range-Doppler surfaces the target was correctly detected in, N_{dets}, vs the total number of range-Doppler surfaces in the scenario, N_{surf}.

$$P_d = N_{dets}/N_{surf} \tag{2}$$

A correct detection decision was made by comparing the detections on each range-Doppler surface to the target GPS ground truth data. If a detection was made at the correct range, known from the target ground truth data, a correct detection decision was made. The ground truth data was recorded at 1 Hz, whereas the radar update rate was 10 Hz, therefore, the ground truth data was first interpolated.

IV. Experimental Results

In this section the results of two radar measurements will be investigated, namely, scenario A and scenario B. Scenario A is a 15 s radar measurement of the car target driving towards the radar, and scenario B is a 10 s measurement of a drone target flying away from the radar. The radar configurations were identical during both scenarios, and an equal number of range-Doppler surfaces, N_{surf}, were formulated in each measurement for each sensor. In scenario A, $N_{surf} = 145$, whereas in scenario B, $N_{surf} = 95$

A. Active and Passive Radar Comparison

Examples of active and PBR range-Doppler surfaces, whilst simultaneously sensing the car target, are presented in Fig. 5. The Doppler axis has been converted to velocity, and identical axis limits have been used to allow direct comparison between the sensors. The active radar's higher resolution in both range and velocity is clearly evident in these figures, though the PBR in Fig. 5b has been included pre-interpolation to provide a better comparison of the sensor performance. The inferior 20 meter range resolution of the PBR results from it's considerably lower IoO waveform bandwidth of 7.61 MHz. In contrast, the active radar has a 30 MHz waveform, resulting in a 5 meter range resolution. The velocity resolution

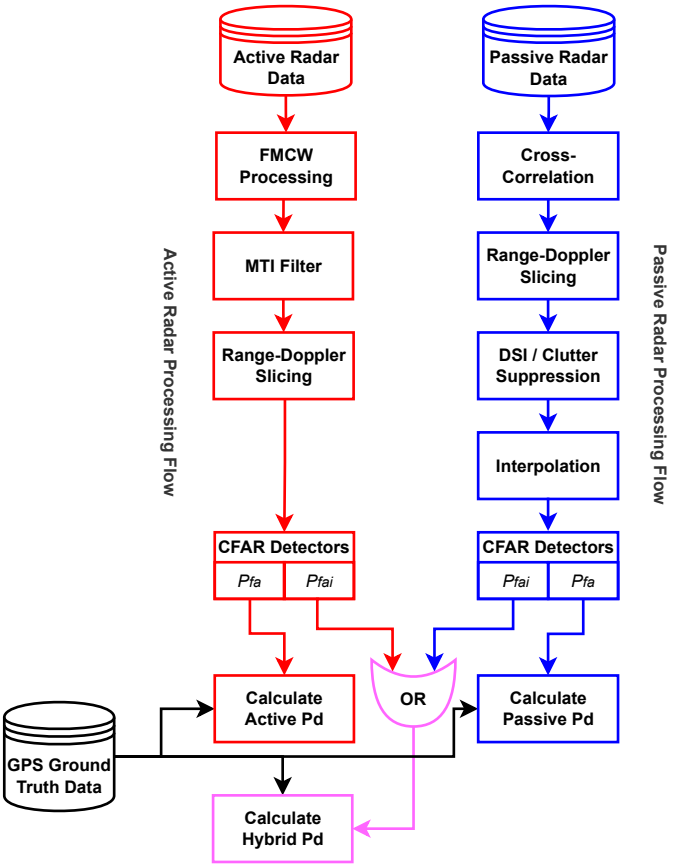

Fig. 4. Radar signal processing flows for the active FMCW sensor (blue) and passive DVB-T bistatic radar sensor (red), operated on the radar data post measurement. Probability of detection was calculated by comparing radar detections to the target ground truth data measured using a GPS logger. The magenta paths represent the hybrid signal processing completed in software post measurement.

is signal processing dependent and determined by the DFT CPI length used when forming the range-Doppler surfaces. The DFT CPI length simultaneously determines the temporal resolution and frequency resolution. The active radar's higher central RF results in a larger Doppler shift for the same target velocity. As such, even for the same PRF and DFT CPI, the velocity cells are smaller in the active radar's range-Doppler surfaces.

B. Hybrid Radar Performance

As discussed in the introduction to this paper, active radar emissions should be minimised when operating covertly. This should be done to lower the probability of the radar transmissions being intercepted by ESMs. In this section, the transmit power of the active radar is reduced to evaluate how the detection performance of the hybrid radar can be sustained. Due to the short-range, and subsequent high SNR, of the targets, both sensors provided a 100% empirical P_d. Therefore, in order to provide a clearer view on the impact of varying the active radar transmit power, the PBR sensor detection performance was first degraded via injecting Additive-White-Gaussian-Noise (AWGN) to the passive radar data. In the case

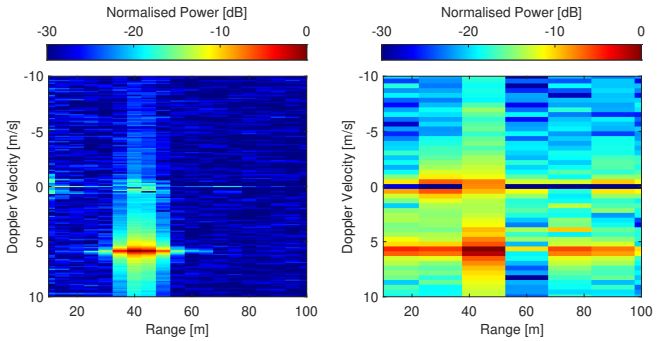

(a) Active radar surface (b) PBR surface

Fig. 5. Comparative range-Doppler surfaces for a car target driving towards the Hybrid radar (a) active S-Band FMCW radar sensor surface; DVB-T PBR sensor surface. These surfaces clearly illustrates the higher resolution of the active radar sensor in both range and Doppler.

of the car scenario, the PBR noise floor was increased by 40 dB, resulting in a P_d of 62.1%. Whereas, in the case of the micro-drone scenario, the PBR noise floor of the PBR was increased by 42 dB, resulting in a P_d of 49.5%. The active radar's transmit power was then reduced by synthetically decreasing the target SNR, equivalent to operating with a lower transmit power. Reductions in SNR were made by increasing the noise floor of the active radar measurement, via injecting AWGN to the active radar data. Eight new transmit power levels were synthetically created between -20 dB and -66 dB. The impact these power reductions would have on the ESM intercept range can be calculated using the one-way radar equation. Given that the only variable that changes is the radar's transmit power P_t, the % reduction in the maximum ESM intercept range, can be easily calculated using,

$$\%Reduction = (1 - \sqrt[2]{P_{t2}/P_{t1}}) \times 100. \quad (3)$$

where P_{t1} is the original radar transmit power, P_{t2} is the new (lower) transmit power. The equivalent reduction in ESM intercept range for each new transmit power level are detailed in Table II. The empirical detection probability results are tabulated in Table II and Table III, and shown in Fig. 6 and Fig. 7, for scenarios A and B respectively. As expected, in general, reducing the active radar transmit power reduces the active radar P_d, initially most significantly in scenario B, due to the considerably smaller RCS of the micro-drone target.

In scenario A, a 32 dB reduction in active radar transmit power results in no degradation in hybrid radar detection performance, yet reduces the ESM intercept range by 97.5%. When the active radar transmit power is further reduced to -40 dB, a greater than 90% detection performance can be sustained through the combination of active and passive sensing. In this case, hybrid sensing provides a 6.9% improvement in detection performance, over the individual sensors, whilst reducing the ESM intercept range by 99%. In scenario A, a peak improvement in detection performance of 8.2% is provided by the hybrid detector.

TABLE II
SCENARIO A - P_d FOR LPI OPERATION WITH CAR TARGET

Active Tx Power (dB)	**-20**	**-26**	**-32**	**-40**	**-46**	**-52**	**-60**	**-66**
ESM Range Decrease (%)	90.00	94.99	97.49	99.00	99.50	99.75	99.90	99.95
Active Radar P_d (%)	100	100	99.3	84.1	55.2	37.2	19.3	5.5
Passive Radar P_d (%)	62.1	62.1	62.1	62.1	62.1	62.1	62.1	62.1
Hybrid Radar P_d (%)	100	100	100	91.0	70.3	64.8	62.1	62.1
Improvement in P_d (%)	0.0	0.0	0.7	6.9	8.2	2.7	0.0	0.0

TABLE III
SCENARIO B - P_d FOR LPI OPERATION WITH DRONE TARGET

Active Tx Power (dB)	**-20**	**-26**	**-32**	**-40**	**-46**	**-52**	**-60**	**-66**
ESM Range Decrease (%)	90.00	94.99	97.49	99.00	99.50	99.75	99.90	99.95
Active Radar P_d (%)	100	84.2	57.9	22.1	17.9	6.3	1.1	0.0
Passive Radar P_d (%)	49.5	49.5	49.5	49.5	49.5	49.5	49.5	49.5
Hybrid Radar P_d (%)	100	85.3	67.4	50.5	49.5	49.5	49.5	49.5
Improvement in P_d (%)	0.0	1.1	9.5	1.1	0.0	0.0	0.0	0.0

In scenario B, the hybrid detector achieved a 67.4% probability of detection after a 32 dB reduction in active radar transmit power. In this case, an improvement in detection performance of nearly 10% is experienced by combining active and PBR detections. Notably, one can observe there is a limited window of active radar transmit powers ($<$ 20 dB) in which the hybrid detector provides a detection enhancement over an individual sensor. Additionally, the detection performance of the hybrid detector never falls below either of the individual sensors. Though this could be possible, due to the requirement to reduce the P_{fa} of the CFAR detectors feeding the hybrid detector. It was, however, calculated that - for a Swerling 1 type target - the energy loss resulting from reducing the P_{fa} from 1×10^{-6} to 0.5×10^{-6}, equates to a negligible energy loss of $<$ 0.3 dB.

C. Adaptive Selection of Active Transmit Power

In the previous two scenarios, it was shown that by combining active and passive radar sensing an increased P_d was achieved. In real world scenarios, the availability, power, and bistatic geometry of the passive IoO will vary, causing the performance of the passive sensor to be dynamic. In order to address this challenge, hybrid radars of the future will require some level of adaptivity to allow the radar configuration to be updated in order to deal with changes in its environment. This adaptivity should inform decisions like when to engage active radar sensing, and at what transmit power. The decision making element will be informed by continually evaluating the radar's performance to ensure it meets a pre-defined performance envelope for a platform to effectively complete its mission. Without this adaptive nature, the full benefits of hybrid radar will likely be unrealisable. By implementing an adaptive process, such as described above, the hybrid radar would be able to dynamically vary the use of the active radar sensor in order to address changes in the environment. The purpose of this may be to minimise the active radar transmissions to lower the probability of the radar being detected by passive radar detection equipment or ESMs, thus the military applications of this adaptive nature are clear. However, there are also civilian applications, due to the now heavily congested electromagnetic environment,

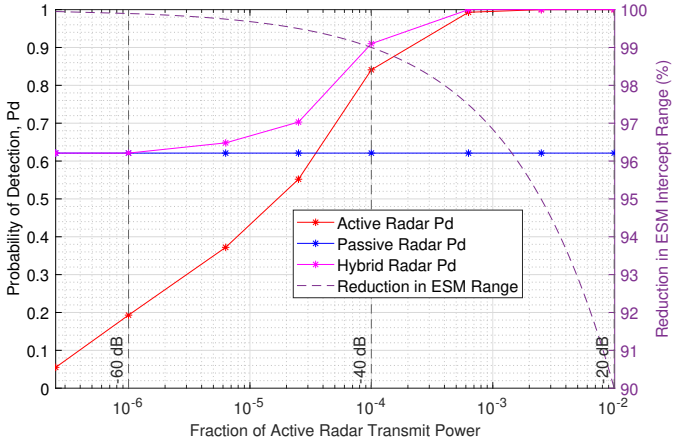

Fig. 6. Scenario A - Active, PBR and hybrid empirical P_d as a function of the active radar's maximum transmit power (left axis). Reduction in ESM intercept range plotted as a function of active radar's transmit power (right axis).

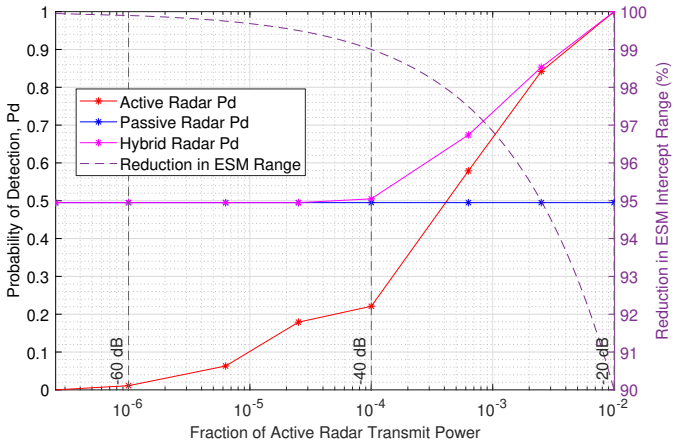

Fig. 7. Scenario B - Active, PBR and hybrid empirical P_d as a function of the active radar's maximum transmit power (left axis). Reduction in ESM intercept range plotted as a function of active radar's transmit power (right axis).

PBR is preferable as it considerably increases the RF spectrum efficiency.

V. Conclusions and Future Work

In this work it has been shown that in both scenarios presented, an improvement in empirical P_d was observed by using hybrid sensing. This was indicated by the the hybrid P_d in many cases exceeding the individual sensor's P_d. Investigation into varying the active radars transmit power, in section IV-B, found that, even at considerably lower power levels, the active sensor still improved the empirical hybrid P_d. This work makes the case for a future research in to hybrid systems that can adaptively vary the active radars transmit power, in order to reach some predefined performance envelope, a theory that is discussed in detail in section IV-C. The results presented in this paper provide clear indications on the benefits of a hybrid radar system. Future work will look to further verify the performance benefits in hybrid radar sensing. Moreover, a two node multistatic hybrid radar experiment is planned, to collect hybrid data for a variety of small-drone targets, permitting further research into information fusion strategies using a greater number of receivers.

Acknowledgment

The authors would like to acknowledge the UK Defence Science and Technology Laboratory (Dstl) for continuing to provide PhD sponsorship for research into active and passive multistatic radar networks and Dilan Dhulashia for his support conducting the hybrid radar experiments.

References

[1] H. Kuschel, J. Heckenbach, and J. Schell, "Deployable multiband passive/active radar for air defense (DMPAR)," *IEEE AES Mag.*, vol. 28, no. 9, pp. 37–45, 2013.

[2] Y. Gao, H. Li, and B. Himed, "Joint transmit and receive beamforming for hybrid active-passive radar," *IEEE Signal Process. Lett.*, vol. 24, no. 6, pp. 779–783, 2017.

[3] F. Wang and H. Li, "Joint waveform and receiver design for co-channel hybrid active-passive sensing with timing uncertainty," *IEEE Trans. on Signal Process.*, vol. 68, pp. 466–477, 2020.

[4] A. Hume and C. Baker, "Netted radar sensing," in *Proc. 2001 IEEE Radar Conf.* IEEE, 2001, pp. 23–26.

[5] G. W. Stimson, H. D. Griffiths, C. J. Baker, and D. Adamy, *Stimson's Introduction to Airborne Radar*, 3rd ed. Edison, NJ: SciTech Publishing, imprint IET, 2014.

[6] T. Brenner, L. Lamentowski, and W. Dyszynski, "Analysis of chosen results based on trials with distributed and collocated passive-active radars," in *Proc. 2018 Int. Conf. Radar*. IEEE, 2018, pp. 1–6.

[7] V. Stejskal, H. Kuschel, T. Brenner, L. Lamentowski, I. Norheim-Naess, P. Samczynski, and J. Kulpa, "DETOUR trials: The mission and its results." German Inst. of Navigation-DGON, 2017, pp. 1–14.

[8] M. Ritchie, N. Peters, and C. Horne, "Joint active passive sensing using a radio frequency system-on-a-chip based sensor," in *Proc. 2022 23rd Int. Radar Symp.*, 2022, pp. 130–135.

[9] P. J. Beasley and M. A. Ritchie, "bladerad: Development of an active and passive, multistatic enabled, radar system," in *Proc. 2021 18th Eur. Radar Conf.*, 2022, pp. 98–101.

[10] M. Ash, M. Ritchie, and K. Chetty, "On the application of digital moving target indication techniques to short-range FMCW radar data," *IEEE Sensors J.*, vol. 18, no. 10, pp. 4167–4175, 2018.

[11] B. Tan, K. Woodbridge, and K. Chetty, "A real-time high resolution passive WiFi Doppler-radar and its applications," in *Proc. 2014 Int. Radar Conf.* IEEE, 2014, pp. 1–6.

[12] H. Kuschel, D. Cristallini, and K. E. Olsen, "Tutorial: Passive radar tutorial," *IEEE AES Mag.*, vol. 34, no. 2, pp. 2–19, 2019.

[13] R. Cardinali, F. Colone, C. Ferretti, and P. Lombardo, "Comparison of clutter and multipath cancellation techniques for passive radar," in *Proc. 2007 IEEE Radar Conf.*, 2007, pp. 469–474.

[14] X. Bai, J. Han, J. Zhao, Y. Feng, and R. Tao, "Clutter cancellation in passive radar using batch-based CLEAN technique," *EURASIP Advances in Signal Process. J.*, vol. 2021, 08 2021.

[15] V. Chernyak, *Fundamentals of Multisite Radar Systems*. Gordon and Breach Science Publishers, 1998.

[16] H. E. Benseddik, B. Cherki, M. Hamadouche, and A. Khouas, "FPGA-based real-time implementation of distributed system CA-CFAR and Clutter MAP-CFAR with noncoherent integration for radar detection," in *Proc. 2012 Int. Conf. on Multimedia Comput. and Syst.*, 2012, pp. 1093–1098.